

4. THE EXTREME 2015/16 EL NIÑO, IN THE CONTEXT OF HISTORICAL CLIMATE VARIABILITY AND CHANGE

MATTHEW NEWMAN, ANDREW T. WITTENBERG, LINYIN CHENG,
GILBERT P. COMPO, AND CATHERINE A. SMITH

Record warm central equatorial Pacific Ocean temperatures during the 2015/16 El Niño appear to partly reflect an anthropogenically forced trend. Whether they reflect changes in El Niño variability remains uncertain.

Introduction. Recent studies have investigated whether both the amplitude and key characteristics of El Niño–Southern Oscillation (ENSO) events have been changing, potentially due to some natural and/or anthropogenic change in the tropical Pacific Ocean state during recent decades (e.g., Yeh et al. 2009; Lee and McPhaden 2010; Newman et al. 2011; McGregor et al. 2013). If so, when might this change be identifiable in individual ENSO events? Was the extreme warmth in the equatorial Pacific seen in the recent 2015/16 El Niño, particularly near the dateline (L’Heureux et al. 2017), a harbinger of this change? To address these questions, we assess this event using statistics of Niño3 (5°N–5°S, 150°–90°W) and Niño4 (5°N–5°S, 160°E–150°W) sea surface temperature (SST) indices, derived from observational datasets and coupled general circulation model simulations. We use two indices to capture differences between events, important to both forecasts and diagnosis of ENSO and its impacts (Compo and Sardeshmukh 2010; Capotondi et al. 2015).

How extreme was the 2015/16 El Niño? We compare the December 2015 (DEC2015) equatorial SST anomaly (SSTA) to the SSTA distribution during 1891–2000, to more stringently test against potentially recent non-stationarity. (Other winter months yielded similar results.) Figure 4.1 shows histograms of monthly ERSST.v5 Niño3 and Niño4 indices, compared with two different probability distribution functions (PDFs) determined not by fitting the histogram, but

by fitting two different Markov processes to each index time series: an AR1 process (or red noise; e.g., Frankignoul and Hasselmann 1977) with a memory time scale on the order of several months, yielding a Gaussian (normal) distribution; and a “stochastically generated skewed” process (SGS; Sardeshmukh et al. 2015), similar to the AR1 process but with noise that is asymmetric and depends linearly on the SSTA, yielding a non-Gaussian (skewed and heavy-tailed) distribution. Confidence intervals for these PDFs are determined from large ensembles of 110-year realizations generated by each process. (See online supplement for details.)

The SGS distribution captures the significant positive skewness of the Niño3 PDF (Fig. 4.1a). The observed tail probability (the probability of Niño3 reaching its observed DEC2015 magnitude) is underestimated by the Gaussian AR1 PDF, but not by the skewed SGS PDF. This result is insensitive to the dataset or to removing the 1891–2015 linear trend. Overall, the SGS distributions suggest that the probability of a monthly Niño3 value reaching or exceeding the DEC2015 magnitude is about 0.5%, consistent with previous occurrences of strong El Niño events in the observational record.

Results are quite different for Niño4, where weak negative skewness (Fig. 4.1b) means that the Gaussian distribution overestimates the DEC2015 tail probability. The DEC2015 Niño4 value was unprecedented in all five datasets, apparently impacted by a secular warming trend. Relative to its linear trend, however, the ERSST.v5 dataset had higher Niño4 values earlier in the record.

How likely was the 2015/16 El Niño? We next evaluate the likelihood and severity of the 2015/16 event relative to the gradually warming background by applying the generalized extreme value (GEV) distribution (e.g., Coles 2001; Ferreira and de Haan

AFFILIATIONS: NEWMAN, CHENG, COMPO, AND SMITH—CIRES, University of Colorado, Boulder, and NOAA Earth Systems Research Laboratory, Physical Sciences Division, Boulder, Colorado; WITTENBERG—NOAA Geophysical Fluid Dynamics Laboratory, Princeton, New Jersey

DOI:10.1175/BAMS-D-17-0116.1

A supplement to this article is available online (10.1175/BAMS-D-17-0116.2)

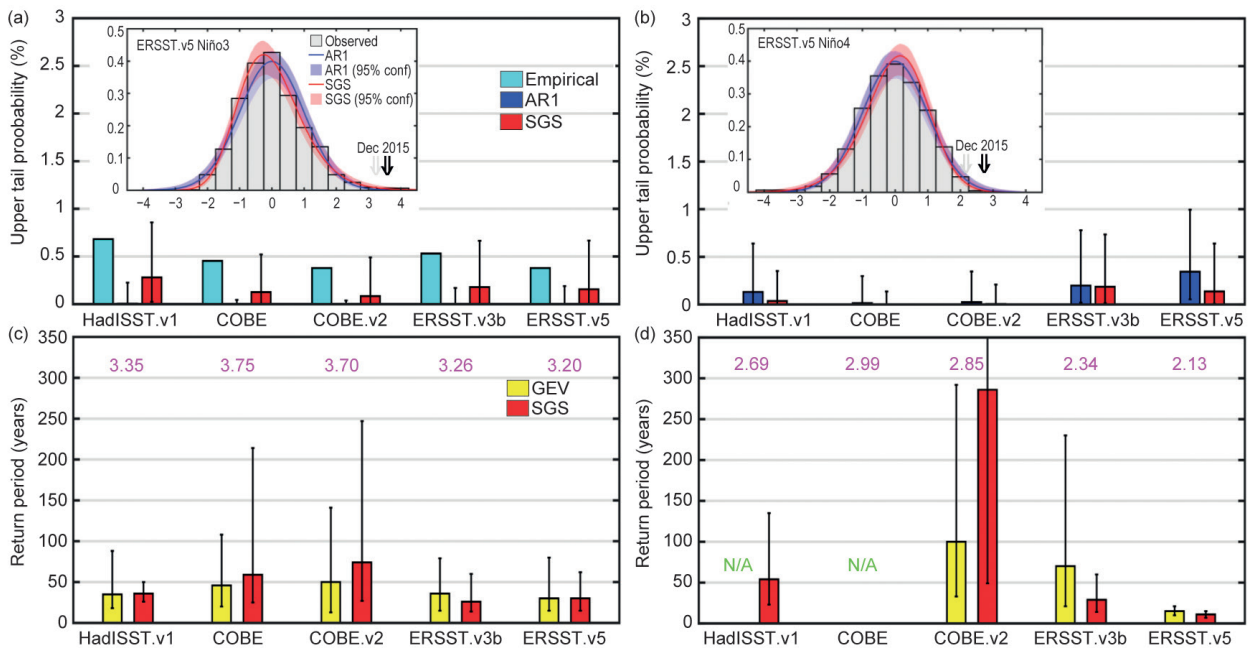


FIG. 4.1. Estimations of DEC2015 (a) Niño3 and (b) Niño4 upper tail probabilities (%). For each SST reconstruction, bars show the scalar tail probability empirically derived from the dataset and also its median value from ARI and SGS distributions; ranges are shown by the whiskers. Insets compare SGS and ARI PDFs with data histograms, using ERSST.v5 values standardized with respect to 1891–2000 (other datasets yielded similar results). Corresponding 95% confidence intervals are shaded; DEC2015 amplitudes are indicated by arrows, where the linear trend is (gray) or is not (black) first removed. Return period estimation (years) of linearly detrended 2015/16 (c) Niño3 and (d) Niño4 indices using the annual maximum of monthly SSTs. For each SST reconstruction, the bars show the 110-year sampling distribution of the return period matching the observed 2015/16 standardized values (magenta numbers), with ranges shown by the whiskers. N/A indicates return periods not derivable using the GEV technique (see text).

2015) to the historical annual maximum of linearly detrended monthly Niño3 and Niño4 indices during 1891–2000. [See online supplement for our Bayesian analysis (Cheng et al. 2014).] The return period, or (re) occurrence probability of an El Niño event with the observed 2015/16 intensity (a “2015/16-level” event), is derived for both indices from each dataset. The same assessment is repeated with the SGS ensembles discussed above.

Our analysis suggests that a 2015/16-level event could be expected for Niño3 roughly once every 40 years. This median return period is reasonably robust to the observational or synthetic SGS dataset used. However, the uncertainty estimates for the return period, and thus the likelihood of the 2015/16 event, are less robust. Both ERSST datasets showed the least uncertainty and shortest return periods, with a 2015/16-level Niño3 SSTA occurring every 5 to 50 years, while COBE2 showed the greatest uncertainty with a range of 10 to 120 years. The SGS distributions, which have more extreme tail events, reduced the return period uncertainty for the ERSST and Had-

ISST.v1 datasets and suggested a greater likelihood of 2015/16-level SSTA extremes.

For Niño4, there is much less agreement among the datasets (Fig. 4.1d), with the return period of a 2015/16-level event lowest for the ERSST datasets. For those datasets where the 2015/16 Niño4 SSTA was unprecedented, the return period cannot be derived using the GEV approach. From ERSST.v5, however, such an event could occur one year in ten.

Was the 2015/16 El Niño impacted by multidecadal trends in equatorial Pacific SST or ENSO variability?

Figure 4.2 illustrates the evolution of 30-year mean SST and 30-year ENSO amplitude over the past 160 years, for two observational reconstructions and two model simulations. For simplicity we discuss only the HadISST.v1.1 and ERSST.v5 reconstructions, which generally bound the behavior of the other products we examined (HadISST.v2, ERSST.v3b, ERSST.v4, COBE, COBE.v2, Kaplan.v2, SODA-si.v3).

For both Niño3 and Niño4, the 1987–2016 epoch was observed to be either the warmest or the second

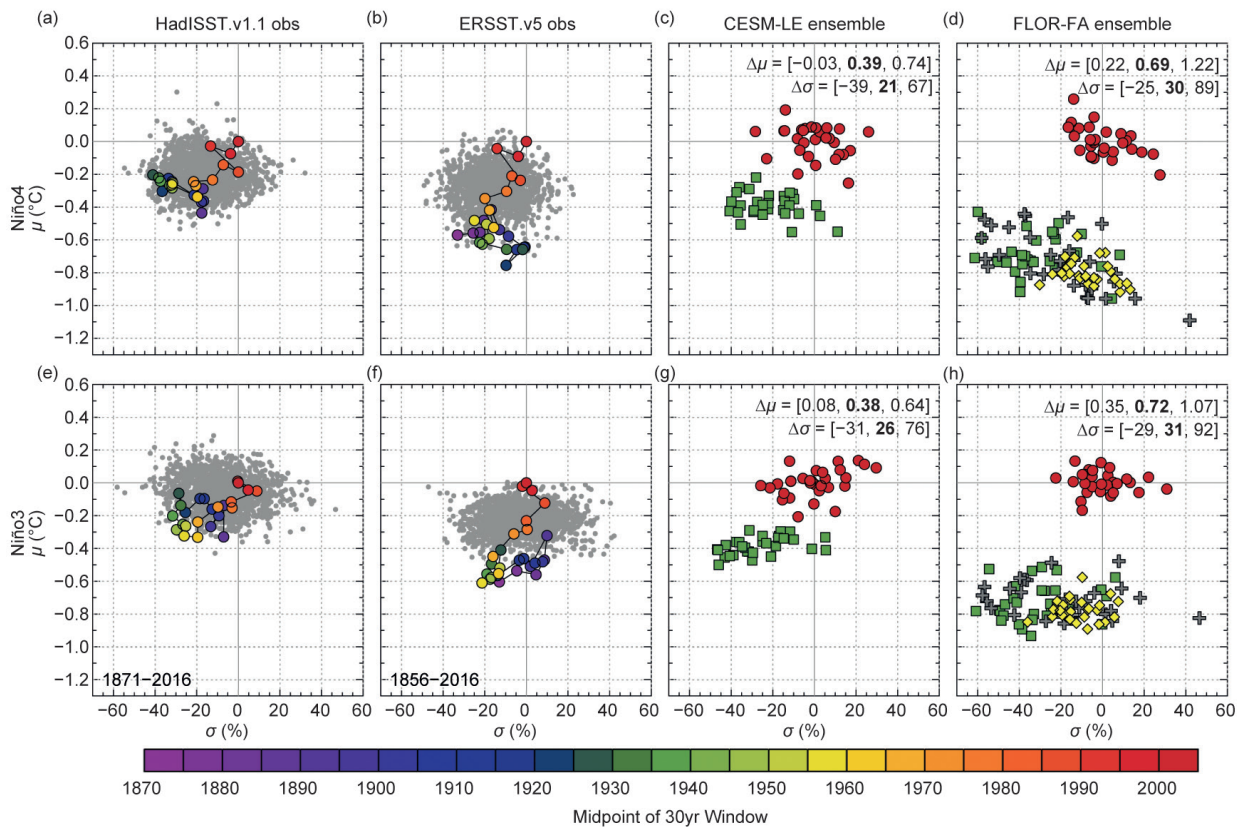


FIG. 4.2. Statistics for annually smoothed SSTs averaged over (a)–(d) Niño4 and (e)–(h) Niño3. Y-axis is the 30-year mean (μ , °C departure from 1987–2016); x-axis is the 30-year std dev (σ , % departure from 1987–2016). (a),(b),(e),(f) sample the observationally reconstructed 30-year statistics every 5 years (colored dots). Gray dots show analogous statistics from 8000-year LIM simulations trained using detrended 1959–2000 data from HadISST.v1.1 or ERSST.v5. (c),(g) show the CESM-LE 30-member ensemble simulation with “ALL” (anthropogenic + natural) historical forcings, for 1987–2016 (red dots) and 1920–49 (green squares) relative to the 1987–2016 ensemble mean; inset indicates ALL ensemble [minimum, average, maximum] change in μ and σ from 1920–49 to 1987–2016. (d),(h) show analogous statistics for the FLOR-FA 30-member ALL ensemble, along with a 30-member “NAT” ensemble with natural forcings only for 1920–49 (gray crosses) and 1987–2016 (yellow diamonds), also relative to the ALL ensemble mean.

warmest 30-year epoch on record, depending on the observational dataset. The warming trend is clearest after 1970 and in Niño4. It is more pronounced in ERSST.v5 than HadISST.v1.1. The centennial warming of both indices is marginally within the bounds of what could be expected from intrinsic multidecadal variations for HadISST.v1.1, but is outside the bounds for ERSST.v5, relative to a statistically stationary multivariate AR1 process [a linear inverse model (LIM), constructed from detrended observed tropical SSTAs during 1959–2000; see online supplement and Newman et al. 2011]. This is consistent with earlier analysis (Solomon and Newman 2012) finding equatorial Pacific 1900–2010 warming trends to be significant near and west of the dateline, despite uncertainty in amplitude.

Robust equatorial Pacific warming from 1920–49 to 1987–2016 is evident in ensemble simulations

from the NCAR CESM-LE and GFDL FLOR-FA global coupled GCMs driven by historical natural and anthropogenic (“ALL”) forcings (Figs. 4.2c,d,g,h). CESM-LE’s warming is compatible with all the reconstructions, though most of its members warm more than HadISST.v1.1 and less than ERSST.v5. FLOR-FA’s warming is strong enough to be detected with any pair of 30-year means drawn randomly from each epoch. It is marginally compatible with ERSST.v5 but not with HadISST.v1.1. The FLOR-FA ensemble simulation with only natural (solar and volcanic, “NAT”) forcings shows ensemble-mean cooling from 1920–49 to 1987–2016, so the FLOR-FA ALL warming must be entirely anthropogenic.

Compared to the historical changes in 30-year mean SST, there is less observational consensus about changes in ENSO SSTA variance. In Niño4, HadISST.v1.1 shows a fairly monotonic 40% amplifi-

cation of ENSO from the 1920s to the present, while ERSST.v5 shows only a 10% amplification and more interdecadal modulation of ENSO amplitude; neither exceeds the expected bounds of intrinsic multidecadal variations. In Niño3, ENSO amplitudes strengthen by 10% in HadISST.v1.1 since 1900, but weaken by 10% in ERSST.v5.

The CESM-LE and FLOR-FA ALL simulations both show ensemble-mean ENSO amplification from 1920–49 to 1987–2016. However, the strong intrinsic interdecadal modulation of ENSO means that some individual realizations experience greater or smaller amplification; a few even weaken. The simulations are broadly consistent with the reconstructed historical changes in ENSO amplitude, but this is primarily due to the reconstruction uncertainty and to intrinsic modulation of ENSO that produces large sampling variability of amplitudes over 30-year epochs (Wittenberg 2009; Newman et al. 2011). Interestingly, the FLOR-FA ALL and NAT simulations both show ENSO amplification (and reduced ENSO modulation) during 1987–2016, mainly because the quietest epochs vanish, suggesting natural forcings are key to the FLOR-FA results.

Conclusions. The 2015/16 El Niño was a strong but not unprecedented warm event in the eastern equatorial Pacific (Niño3), comparable to events occurring every few decades or so. However, central equatorial Pacific (Niño4) 2015/16 warmth was unprecedented in all SST reconstruction datasets except ERSST.v4. This exceptional warmth was unlikely, although not impossible, to have occurred entirely naturally, and appears to reflect an anthropogenically forced trend.

Whether this extreme warmth was associated with a change in ENSO variability, however, is less clear, given the substantial disagreement between datasets including uncertainty in their anthropogenic trend estimates (Deser et al. 2010; Solomon and Newman 2012). Interestingly, SST reconstructions with relatively higher Niño3 and Niño4 variances around the start of the 20th century (e.g., ERSST.v5) are also based on newer ICOADS releases, which include additional observations during that time (Freeman et al. 2016). Moreover, equatorial Pacific sea level pressure variance (i.e., Darwin and Tahiti) shows no pronounced centennial increase (e.g., Torrence and Compo 1998). Finally, our model results illuminate, but do not reconcile, continuing disparities among climate models concerning anthropogenic impacts on ENSO variability (Collins et al. 2010; Watanabe et al. 2012; Capotondi et al. 2015) due to lingering dynamical

biases in the models (Bellenger et al. 2014; Graham et al. 2017). These issues suggest that we cannot yet confidently detect whether a secular change in ENSO variability (apart from the background warming) has occurred over the past century. Our study thus highlights the need to further reduce uncertainty in observational reconstructions, and further improve dynamical models, to better gauge future ENSO risks.

REFERENCES

- Bellenger, H., E. Guilyardi, J. Leloup, M. Lengaigne, and J. Vialard, 2014: ENSO representation in climate models: From CMIP3 to CMIP5. *Climate Dyn.*, **42**, 1999–2018, doi:10.1007/s00382-013-1783-z.
- Capotondi, A., and Coauthors, 2015: Understanding ENSO diversity. *Bull. Amer. Meteor. Soc.*, **96**, 921–938, doi:10.1175/BAMS-D-13-00117.1.
- Cheng, L., A. AghaKouchak, E. Gilleland, and R. W. Katz, 2014: Non-stationary extreme value analysis in a changing climate. *Climatic Change*, **127**, 353–369, doi:10.1007/s10584-014-1254-5.
- Coles, S., 2001: *An Introduction to Statistical Modeling of Extreme Values*. Springer, 209 pp.
- Collins, M., and Coauthors, 2010: The impact of global warming on the tropical Pacific Ocean and El Niño. *Nat. Geosci.*, **3**, 391–397, doi:10.1038/ngeo868.
- Compo, G. P., and P. D. Sardeshmukh, 2010: Removing ENSO-related variations from the climate record. *J. Climate*, **23**, 1957–1978, doi:10.1175/2009JCLI2735.1.
- Deser, C., A. S. Phillips, and M. A. Alexander, 2010: Twentieth century tropical sea surface temperature trends revisited. *Geophys. Res. Lett.*, **37**, L10701, doi:10.1029/2010GL043321.
- Ferreira, A., and L. de Haan, 2015: On the block maxima method in extreme value theory: PWM estimators. *Annals of Statistics*, **43**, 276–298, doi:10.1214/14-AOS1280.
- Frankignoul, C., and K. Hasselmann, 1977: Stochastic climate models. Part II: Application to sea-surface temperature anomalies and thermocline variability. *Tellus A*, **29**, 289–305.
- Freeman, E., and Coauthors, 2016: ICOADS Release 3.0: A major update to the historical marine climate record. *Int. J. Climatol.*, **37**, 2211–2232, doi:10.1002/joc.4775.
- Graham, F. S., A. T. Wittenberg, J. N. Brown, S. J. Marsland, and N. J. Holbrook, 2017: Understanding the double peaked El Niño in coupled GCMs. *Climate Dyn.*, **48**, 2045–2063, doi:10.1007/s00382-016-3189-1.

- L'Heureux, M. L., and Coauthors, 2017: Observing and predicting the 2015/16 El Niño. *Bull. Amer. Meteor. Soc.*, **98**, 1363–1382, doi:10.1175/BAMS-D-16-0009.1.
- Lee, T., and M. J. McPhaden, 2010: Increasing intensity of El Niño in the central-equatorial Pacific. *Geophys. Res. Lett.*, **37**, L14603, doi:10.1029/2010GL044007.
- McGregor, S., A. Timmermann, M. H. England, O. Elisa Timm, and A. T. Wittenberg, 2013: Inferred changes in El Niño–Southern Oscillation variance over the past six centuries. *Climate Past*, **9**, 2269–2284, doi:10.5194/cp-9-2269-2013.
- Newman, M., S.-I. Shin, and M. A. Alexander, 2011: Natural variation in ENSO flavors. *Geophys. Res. Lett.*, **38**, L14705, doi:10.1029/2011GL047658.
- Sardeshmukh, P. D., G. P. Compo, and C. Penland, 2015: Need for caution in interpreting extreme weather statistics. *J. Climate*, **28**, 9166–9187, doi:10.1175/JCLI-D-15-0020.1.
- Solomon, A., and M. Newman, 2012: Reconciling disparate twentieth-century Indo-Pacific ocean temperature trends in the instrumental record. *Nat. Climate Change*, **2**, 691–699, doi:10.1038/nclimate1591.
- Torrence, C., and G. P. Compo, 1998: A practical guide to wavelet analysis. *Bull. Amer. Meteor. Soc.* **79**, 61–78, doi:10.1175/15200477(1998)079<0061:APGTWA>2.0.CO;2.
- Watanabe, M., J.-S. Kug, F.-F. Jin, M. Collins, M. Ohba, and A. T. Wittenberg, 2012: Uncertainty in the ENSO amplitude change from the past to the future. *Geophys. Res. Lett.*, **39**, L20703, doi:10.1029/2012GL053305.
- Wittenberg, A. T., 2009: Are historical records sufficient to constrain ENSO simulations? *Geophys. Res. Lett.*, **36**, L12702, doi:10.1029/2009GL038710.
- Yeh, S.-W. J., S. Kug, B. Dewitte, M.-H. Kwon, B. P. Kirtman, and F.F. Jin, 2009: El Niño in a changing climate. *Nature*, **461**, 511–514, doi:10.1038/nature08316